Brake System Design for Sports Cars using Digital Logic Method

S.Ebrahimi-Nejad*, M.Kheybari

Vehicle Dynamical Systems Research Lab, School of Automotive Engineering, Iran University of Science and Technology, Tehran, Iran

ebrahiminejad@iust.ac.ir

Abstract

Brake system performance significantly affects safety, handling and vehicle dynamics. Therefore, the objective of this paper is to discuss brake system characteristics and performance and component design parameters. We perform a detailed study of a specific brake system designed for Mercedes-AMG SLC-43, considering component design parameters and operational points, and finally conduct the vehicle braking system layout design. To this end, brake force and torque calculations and power dissipation modelling is performed. Then, ventilated brake discs are designed for the front and rear brakes. A main goal of the present article is to apply digital logic method to the material selection procedure among the candidate material proposed for brake components and rank the materials according to performance indices. The performance indices of five candidate materials were calculated and compared to select the best option for application in the brake disc. Finally, the calculations of the brake pedal, booster, cylinder, hoses and tubes are obtained.

Keywords: *Brake system design; Disc; Digital logic; Mercedes-AMG; Pads; Vehicle*

[Downloaded from ce.iust.ac.ir on 2026-06-14]

[DOI: 10.22068/ijae.7.4.2571]

1. Introduction

Vehicle brake system is regarded as an energy dissipation device, which converts kinetic energy (momentum) into thermal energy (heat). The main function of the brakes is speed control, and the rate of energy dissipation defines the vehicle's deceleration rate. After pressing the pedal or applying the handbrake, the car transmits the input force of the driver's foot or hand all the way to the brake pads. However, the final stopping force is actually many times more powerful than the car's driving force. As brake pads need to be pressed by a much greater force than any driver could apply, the elements of the braking system must amplify the force exerted by the driver's foot.

It is worth mentioning that in addition to the fundamental equipment of the braking system, nowadays, numerous auxiliary control and assistive systems have been embedded in the braking system to assist the driver in sensitive and challenging driving situations as well as to offer to the driver more comfort in urban driving conditions. For example, brake distribution factor can be dynamically regulated under variable loading conditions when cornering and accelerating to help distribute braking torque more efficiently to the wheels with greater grip, to improve traction and handling and braking. Additionally, a so-called HOLD feature is provided to assist the driver in heavy traffic or when stopping on a slope, which the keeps the brakes applied without keeping the driver's foot on the brake pedal.

According to different working conditions, especially the conditions of heat transfer in the brakes [1], modern cars are equipped with either of two different types of brake system designs, namely, disc brakes and drum brakes (Figure 1). Nowadays, most cars are equipped with disc brakes on front wheels, while a significant percentage of cars still use rear drum brakes. Therefore, a brake system of a typical car consists of front disc brakes and either drum or disc rear brakes along with a connecting system, which links brake calipers to the master and slave cylinders.

The main types of drum brakes include: simplex, duo-trailing shoe brakes, duplex, duo-duplex, uni-servo, and duo-servo drum brakes. The main components of drum brakes include: brake drum, expander, pull back springs, back plate, shoes and friction linings, and anchor pins.

Various aspects such as heat transfer, the reliability of system components, and noise and vibrations are vital in the design of the brake system, and should receive special attention in this process. Talati and Jalalifar [1] studied brake system heat transfer and solved the time and space dependent governing equations for disc and pad transient heat conduction. Ganji and Ganji [2] studied the brake squeal phenomenon in terms of the frequency and amplitude of limited cycle oscillations using Stribeck friction model and considering nonlinear equations of motion as a result of large deformations. Phatak and Kulkarni [3] studied the parameters affecting drum brake noise, and achieved squeal noise reduction through structural modification and stiffening of drum brake backplate. Romero and Queipo [4] compared the buckling and stress analyses of brake pedal designs performed using deterministic and reliability-based (probabilistic) design optimization models through a risk allocation analysis. Although deterministic design optimization is more wide-spread in the industry, their results indicated that for the same probability of system failure, when compared to deterministic design optimization, the reliability-based design optimization brake pedal design was lighter and more robust (less mass variable) [4].

This paper investigates the brake system component design parameters and design characteristics of a braking system based on brake system performance. We perform a detailed study of a specific brake system designed based on the data and specifications of Mercedes-AMG SLC-43 [5] based on standards and regulations [6]. Various material selection schemes are studied and reviewed [7-12] to enable an optimized selection procedure. A main goal of the article is to apply digital logic method to the material selection procedure among the candidate material proposed for brake disc application and rank the materials according to performance indices.

The remainder of the paper is arranged as follows. Design and material selection methodology and formulations are described in Section 2. Results and research findings are discussed in Section 3. Finally, concluding remarks and directions for future investigations are presented in Section 4.

2. METHODS AND MATERIALS

Performance of vehicle brake system can effectively reduce the temperature rise of various brake system components and brake fluid vaporization [1], unwanted noise and vibrations, brake pad fade and malfunction of the brakes.

In drum brakes, after pressing the pedal, the expander expands the shoes, pressing them by the drum, so that friction forces are generated at the interfaces of the brake drum and the curved friction linings. Releasing the pedal, releases the brakes and the pullback spring withdraws the shoes, thus allowing the wheels to rotate freely, again. In disc brakes, a metal or composite disc and one or more flat brake pads, which may be located on either sides of the disc, replaces the drum assembly. In disc brake systems, when the driver presses the pedal, the fluid from the master cylinder forcefully moves the plastic or metallic pistons toward the disc, hence, squeezing the friction pads onto the rotating disc to stop the car.

In order to perform an appropriate design of the braking system, we used real data from Mercedes-AMG SLC-43. Table 1 shows the main specifications of tire, wheel and brake system of the selected vehicle. The main brake components of the vehicle, including the ventilated brake disc, friction pads and caliper are shown in Figure 2.

The design of the basic braking system parameters will be performed based on vehicle dimensions, weights and configurations, which are listed in Table 2.

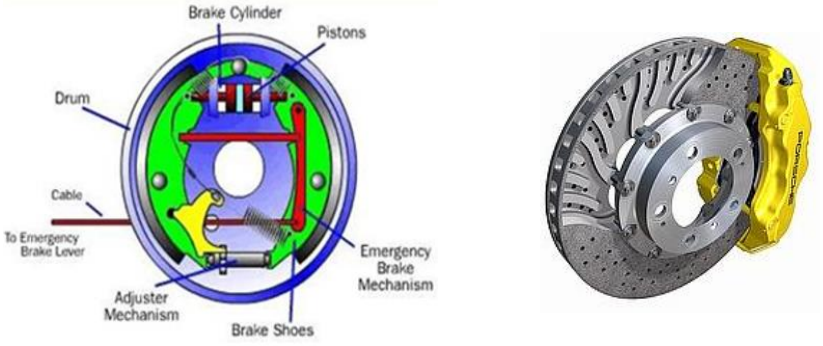

(a) (b)

Fig1. a) Drum brake, b) Disc brake

Table 1. Specifications of tire, wheel and brake system [5]

[Downloaded from ce.iust.ac.ir on 2026-06-14]

[DOI: 10.22068/ijae.7.4.2571]

Component	Material/Size
Front and rear rim	Aluminum
Front tire	235 / 40 R18
Rear tire	255 / 35 R18
Front and rear brakes	Ventilated disc

Table 2. Dimensions and weights of Mercedes-AMG SLC-43 [5]

Dimension and weight	value
Vehicle length	4143 mm
Vehicle height	1797 mm
Vehicle width	2006 mm
Wheelbase	2431 mm
Turning circle	10.52 mm
Track width front	1559 mm
Track width rear	1565 mm
Maximum speed	280 km/h
Curb weight	1595 kg
Gross vehicle weight	1890 kg

Fig2. The ventilated brake disc, pads and caliper of SLC-43 [5]

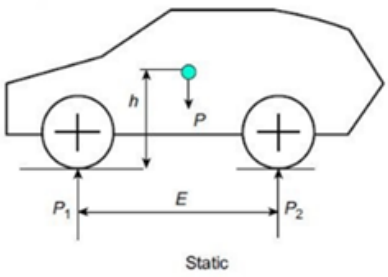

Fig3. Static road vehicle force system [6]

[Downloaded from ce.iust.ac.ir on 2026-06-14]

[DOI: 10.22068/ijae.7.4.2571]

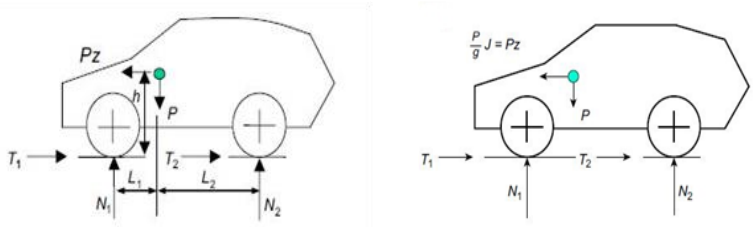

Fig4. 2D car model on a horizontal road in dynamic braking conditions a) dimensions, b) forces [6]

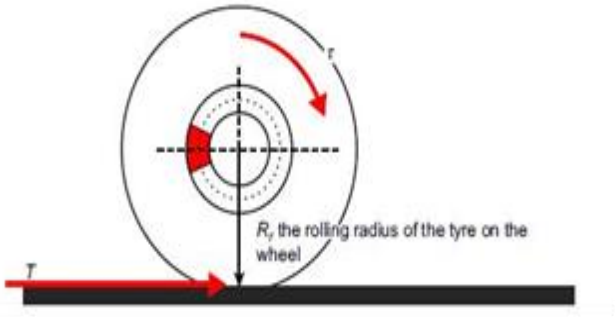

Fig5. Disc brake on road wheel showing the braking force at the tire/road interface [6]

2.1 Brake Force and Torque Calculations

Throughout the calculations, the front axle is noted with subscript 1 and the rear axle is shown with subscript 2. Static conditions of the vehicle is shown schematically in Figure 3, in which h and E are the height of the center-of-mass and the wheelbase, respectively.

To perform axle load calculations in static conditions, we take moments about the instantaneous point of contact of the front and rear wheels with the road, to give P_1 and P_2:

$$P_1 = \frac{PL_2}{L_1+L_2} = \frac{PL_2}{E}$$

$$P_2 = \frac{PL_1}{L_1+L_2} = \frac{PL_1}{E}$$

in which P is the vehicle total weight (mg) and P_1 and P_2 are the static loads on the front and rear axles, and L_1 and L_2 are the longitudinal distance of the front and rear axles from the vehicle's center-of-mass, respectively.

Now, we consider dynamic braking mode, as shown in Figure 4, for which the braking acceleration is replaced by inertia force, according to D'Alembert's principle.

Axle normal loads are calculated in dynamic braking conditions by taking moments about the contact point of the front and rear wheels. We assume a braking deceleration of J and define the rate of braking as $z = \frac{J}{g}$, therefore, the total braking force is $mJ = \frac{P}{g}j = Pz$ and dynamic normal axle loads Ni can be calculated as:

$$N_1 = \left(\frac{L_2}{L_1+L_2} + \frac{zh}{L_1+L_2}\right)P$$

$$N_2 = \left(\frac{L_1}{L_1+L_2} - \frac{zh}{L_1+L_2}\right)P$$

The ratio of braking forces in front and rear axles, considering the situation in which both wheels become locked at the same time, can be calculated as:

$$X_i = \frac{N_i}{P}$$

subject to the constraint $X_1 + X_2 = 1$, and the brake force distribution ratio (X_1/X_2) can be determined.

Now for a critical braking rate of $Z_{critical} = 0.6$, we can calculate the brake force distribution ratio and the dynamic normal axle loads N_i from Equations 3 and 4 for driver-only weight (DOW) and also for gross vehicle weight (GVW). Next, we calculate longitudinal load transfer:

[Downloaded from ce.iust.ac.ir on 2026-06-14]

[DOI: 10.22068/ijae.7.4.2571]

$$p_f = p_1 + \frac{mJh}{E}$$

$$p_r = p_2 - \frac{mJh}{E}$$

Then, to calculate the maximum braking torque of each wheel, first, we calculate the rolling (or dynamic) radii of the front (r_{r_F}) and rear (r_{r_R}) tires based on wheel and tire data presented in Table 1:

$$r_r = \frac{25.4}{2}(D) + 0.923(W)\frac{H}{W}$$

For the front tires, wheel rim diameter is D=18 inch, W=235 mm, and H/W=40% and for the rear tires, D=18 inch, W=255 mm, and H/W=35%. Assuming no lateral variation in brake torque, the axle braking force T_i at the tire/road interface is generated by two brakes, so for each wheel on the axle the brake torque τ_{wi} is calculated from the braking force of the wheel (T_{wi}), as illustrated in Figure 5. The maximum torque is calculated from Equation 9:

$$\tau_{wi} = T_{wi}\, r_{ri} = \frac{X_i\, PZ\, r_{ri}}{2}$$

2.2 Maximum Brake Power Dissipation

After calculating the maximum wheel braking torque, the energy dissipation rate is calculated:

$$\dot{Q}_i = T_{wi}\, \omega$$

where ω is the instantaneous angular velocity (rotational speed), which is calculated at 90% maximum vehicle speed V_{max} as:

$$\omega_i = \frac{0.9 \times V_{max}}{r_{r_i} \times 3.6}$$

The amount of dissipated energy per wheel on each axle is calculated as:

$$Q_i = \frac{1}{2}\left(\frac{mV^2 Xi}{2}\right)$$

Disc brakes with ventilated rotors are now almost universally used on the front axles of passenger cars and light commercial vehicles because of their ability to dissipate more heat than solid rotors, especially at higher speeds. On the rear axles of these vehicles, either drum brakes or solid disc brakes can be used. For the vehicle studied in this article (AMG-SLC43), disc brakes are used for all of the wheels.

2.3 Design of Ventilated Disc Brake

In disc brakes, the inner radius (r_i) of the disc is limited to the wheel hub assembly and the outer radius (r_o). However, to minimize the effect of pad wear on its effective radius, Day [6] suggested that good practice for the inner to outer radius ratio of the disc is $r_o/r_i \leq 1.5$. Therefore, the inner and outer radii of the disc are assumed such that this condition is satisfied. The mean (effective) radius of the disc brake is calculated as:

$$r_e = r_m = (r_o + r_i)/2$$

A disc brake is illustrated in Figure 6, which shows an idealized sector-shaped brake pad in contact with one side of the friction ring of a brake disc superimposed on an image of an actual brake disc and pad [6]. As the disc rotates, its surface sweeps under the stationary disc brake pad and the 'swept area', 'rubbing path' or 'friction surface area' of the disc is calculated from the outer and inner radii, which bound the swept area. This part of the disc is often called the 'friction ring', and the part of the disc that connects the friction ring to the wheel hub is often called the 'top hat' section.

Friction surface area of the disc can be calculated:

$$A_s = \pi(r_o^2 - r_i^2)$$

Considering a certain length for the pad and also the friction surface area of the disc, we can calculate the torque generated by the brake disc at the pad/disc interface where we have (sliding) friction and μ is the coefficient of sliding friction between the pad friction material and the disc. Assuming two brake pads on each wheel, and N_{c1} and N_{c2} being the inner and outer pad clamp forces, respectively, the friction drag force acting on the pads are $F_1 = \mu N_{c1}$ and $F_2 = \mu N_{c2}$ and we can calculate the torque τ_w generated by a disc brake as:

$$\tau_w = \mu(N_{c1} + N_{c2})r_e$$

Assuming that $N_{c1} = N_{c2} = N_c$, the wheel brake torque τ_w generated in a disc brake is:

$$\tau_w = 2\mu N_c r_e$$

We know that $N_c = P_a$, where P_a is the actuation pressure, hence, we can write:

$$\tau_w = 2\mu P_a r_e$$

Although the classical definition of brake factor (BF) is regarded as the ratio of the total friction force generated by the brake stators to the total actuation force applied to the brake stators, disc brake factor is

[Downloaded from ce.iust.ac.ir on 2026-06-14]

[DOI: 10.22068/ijae.7.4.2571]

now usually quoted as $BF = \eta C^* = 2\mu$, which leads to:

$$T_w = BF\ P_a r_e / r_r$$

The total axle braking force is calculated as:

$$T_i = 2\ BF\ P_a r_e / r_r$$

and the total vehicle braking force is:

$$T = 2\ \eta C^*\ P_a r_e / r_r$$

For a hydraulically actuated disc brake, the actuation force P_a applied to a single pad is:

$$P_a = (p - p_t) A_a \eta$$

where p is the hydraulic line pressure (MPa), p_t is the threshold pressure (MPa), and η is the efficiency of the hydraulic actuation system. Assuming that the pad actuation force (P_{ai}) is the same as the clamp force at the pad/disc interface (N_{ci}), combining Equations (17) and (20) gives the wheel brake torque (τ_w):

$$\tau_w = 2\mu\ (p - p_t) A_a \eta\ r_e = BF\ (p - p_t) A_a \eta\ r_e$$

and the axle brake torque (τ_{axle}):

$$\tau_{axle} = 4\mu\ (p - p_t) A_a \eta\ r_e$$

Assuming the efficiency of the hydraulic actuation system η=0.95, the disc brake factor of $BF = \eta C^* = 2\mu$, friction coefficient μ, threshold pressure p_t = 0.8 bar (0.08 MPa), and hydraulic line pressure p=85 bar (8.5 MPa), the actuation force P_a and axle brake torque τ_{axle} is calculated.

2.4 Digital Logic (DL) Method in Brake Disc Material Selection

Reduction of greenhouse gas emissions is a global concern of high significance, especially for the transport industry, which has caused wide-spread use of aluminum alloys in the automotive industry in recent years. This trend shows great potentials for aluminum-alloy-based metal matrix composites (MMCs). Advanced aluminum alloys perform better under severe service conditions which are increasingly being encountered in modern sports vehicles. They have a higher thermal conductivity and lower density compared to gray cast iron and carbon steel which are conventionally used in disc brakes and bring about a significant weight reduction and better heat dissipation in brake discs.

Material selection chart is a very useful tool in comparing a large number of materials at the *concept design* phase which could reflect the fundamental relationships among important material properties and be used to find out a range of materials suitable for a particular application [7]. Generally, the material selection process is performed based on performance indices in the material selection chart [8]. As an alternative approach, digital logic method has been occasionally used for certain engineering application [9]. In order to select an appropriate material for a particular application, the designer can use materials handbook, or international standard sources. Although, knowledge-based system for selecting and ranking the materials for a particular application are available in literature [10, 11], however, information on the application of material selection methods for the design of automotive brake disc is scare. Here, our main purpose is to apply a suitable material selection method to select the best candidate material for brake disc application and to rank the materials according to performance indices. Five candidate materials including grey cast iron (GCI), titanium alloy (Ti-6Al-4V), titanium matrix composite (7.5 wt% WC and 7.5 wt% TiC reinforced composite, TMC), and two types of aluminum matrix composites, namely AMC1 (Al-composite reinforced with 20% SiC) and AMC2 (Al-Cu alloy reinforced with 20% SiC) are studied.

The digital logic method is employed for optimum material selection using comparative ranking of material properties. As a first step, important material property requirements for a brake rotor are determined. In the present study N=5 materials properties, including compressive strength, friction coefficient, wear resistance, thermal capacity and density were selected. A list of candidate materials is given in Table 3, along with their material properties.

The next step is to compare these properties mutually, where and a value of 1 is assigned to the property of higher relative importance and is a value of 0 is assigned to the property with lower relative importance. Therefore, the overall number of judgements are $N(N-1)/2 = 10$. The total score assigned to each material property is calculated and divided by the sum of total scores (equal to the overall number of judgements), which gives the respective weight factor (α_i) of each material property.

Then, the values of the material properties are scaled based on their corresponding weight factor (α_i) and the scaled values (β_i) which is calculated using material property values listed in Table 3. In the case of brake discs, materials with higher specific heat capacity, friction coefficient, and compressive strength are more desirable and their maximum value is given a score of 100 and other values of the material properties are scaled according to the following:

[Downloaded from ce.iust.ac.ir on 2026-06-14]

[DOI: 10.22068/ijae.7.4.2571]

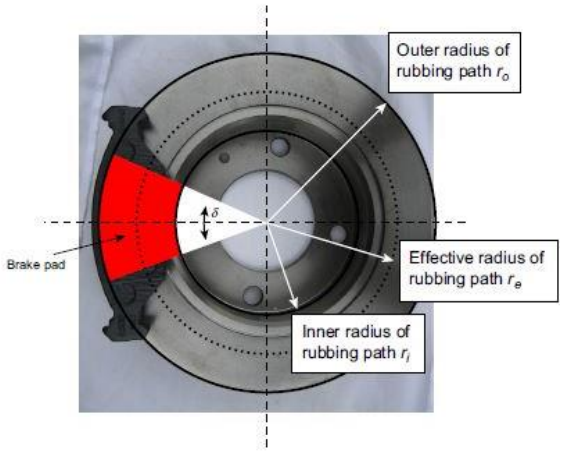

Fig6. Disc Brake Showing the Pad as a Sector on the Rubbing Path [6]

Table 3. Selected material properties of brake disc candidate materials [12]

Properties	**1**	**2**	**3**	**4**	**5**
Material	Compressive Strength (MPa)	Friction coefficient (μ)	Wear rate (10^{-6}mm^3/ Nm)	Specific heat C_p (KJ/Kg.K)	Density (ton/m^3)
GCI	1293	0.41	2.36	0.46	7.20
Ti-6A1-4V	1070	0.34	2.46	0.58	4.42
TMC	1300	0.31	8.19	0.51	4.68
AMC1	406	0.35	3.25	0.98	2.70
AMC2	761	0.44	2.91	0.92	2.80

$$\text{Scaled value} = \frac{\text{Numerical value of the material property} * 100}{\text{Maximum value}}$$

On the other hand, lower values of density and wear rate are more desirable in the design of automotive brake disc, therefore, their minimum value is given the score of 100 and other values are scaled using Equation 25:

$$\text{Scaled value} = \frac{\text{Minimum value} * 100}{\text{Numerical value of the material property}}$$

Finally, material selection is done by calculating material performance index (γ), using the scaled values (βi) and the weight values (αi) performance index, summing over the N selected material properties:

$$\gamma = \sum_{i=1}^{N} \beta_i \alpha_i$$

It is worth noting that this material selection procedure is done without regard to the cost and only accounts for technical capabilities of the material.

2.5 Design of Brake Pedal

The brake pedal, location where force is applied, bearing, support and its spring are shown in Figure 7. According to EEC 71320 regulation, maximum input power (force) that driver can apply to the pedal during braking is 500 N, however, but is important that we also consider a minimum input force of 100 N at the pedal. Moreover, according to ISIRI2992 standard, in the design of hydraulic brake systems, the maximum tolerable amount of pressure exerted on the brake hoses may not exceed 5000 psi.

The forces and moments exerted onto the pedal by the driver's leg and the forces amplified through the pedal lever are important, as they are transmitted to the booster. In order to supply the torque used to generate the angular acceleration of the pedal and

[Downloaded from ce.iust.ac.ir on 2026-06-14]

[DOI: 10.22068/ijae.7.4.2571]

overcome the spring force govern the input force of the pedal through the following Equation:

$$F_{in} = \left(aF_p - K_p\theta - I_p\ddot{\theta}\right)/b \cong \left(aF_p\right)/b$$

By determining the maximum input force, according to the above-mentioned standard, the force transmitted to the booster can be calculated using the geometry of the brake lever which are selected to be a = 36 cm and b = 8.40 cm.

2.6 Booster Calculations

During the engine operation, when the brake is not applied, air inside the casing is sucked by the engine causing partial vacuum of about 500 mm-Hg. Vacuum is also present on the other side of the diaphragm through a valve and pressure is the same on both sides of the diaphragm (Figure 8).

During braking, by applying force on the pedal, pressure difference is created on the two sides of the diaphragm, and an additional force F'_d is exerted on the plate according to Equation 28. Fd is equal to $F'_d - F$, and where the efficiency of booster is η=0.95 we can calculate disc pressure and total input forces from Equations 29 and 30, respectively:

$$F'_d = \eta(A_d - A)(P_{amb} - P_{inlet\ duct})$$

$$P_{disc} = F_d/(\pi(D_o^2 - D_i^2)/4)$$

$$F'_{in} = (\pi D_i^2)/4) \times P_{disc}$$
$$F_{in} = F'_{in} + F_{s1} + F_{s2}$$

in which Fs1 and Fs2 are the booster's two spring forces and Fin is the total input forces. Now we can design the booster by calculating Do and Di from the available information about ro and ri. The boost factor B is calculated from Equation 31:

$$B = \frac{F_{out}}{F_{in}} \cong \frac{F_d + F_{in}}{F_{in}} = \frac{F_d + A_i\frac{F_d}{A_o - A_i}}{A_i\frac{F_d}{A_o - A_i}} = \frac{A_o}{A_i}$$

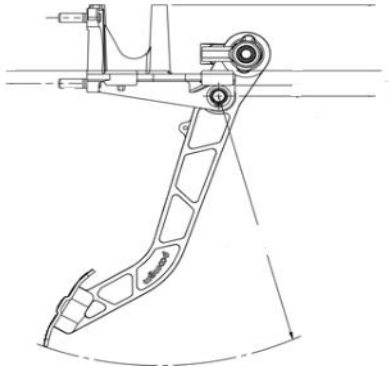

Fig7. Brake pedal schematic representation

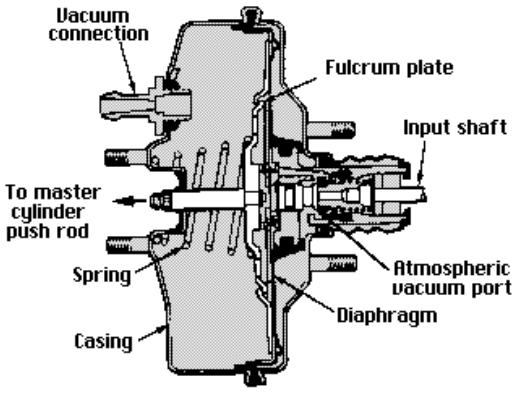

Fig8. Vacuum power brake booster

[Downloaded from ce.iust.ac.ir on 2026-06-14]

[DOI: 10.22068/ijae.7.4.2571]

2.7 Design of Cylinder, Hoses and Tubes

The governing equations for the cylinder are derived, considering that braking force is first transmitted from the booster to the main cylinder and then goes to front and rear wheel cylinders. So, we start with the stroke (maximum displacement) of the main cylinder piston:

$$stroke = \frac{X_{p_{max}}}{R_p}$$

where $X_{p_{max}}$ is the maximum amount of pedal movement and R_p is ratio of brake pedal leverage. The relation between the inlet pressure to the main cylinder and its input forces is:

$$P = (P_{mc} Q_{mc})/A_{mc}$$

in which Q_{mc} is the amount of energy loss caused by friction, the value of which is 95%, A_{mc} is the main cylinder's surface are and P_{mc} is input force. The magnitude of input forces can be calculated as:

$$P_{mc} = R_p F_d F_p$$

Both minimum and maximum values of Pmc can be calculated for a minimum pedal input force of 100 N and a maximum pedal force of 500 N, respectively. The brake pedal leverage ratio was Rp = 3.5, as discussed in Section 3.5. Now, we can calculate the maximum amount of pressure produced by the main cylinder:

$$P = (R_p F_d F_p Q_{mc})/A_{mc}$$

Volume variations caused by deformation of caliper and squeezing the brake pads can be estimated according to empirical studies, as a function of the compression ratio of brake pads Cbp. In order to check whether the size of the slave (wheel) cylinder is suitable for the present brake system and in accordance with the master cylinder, the master to slave cylinder ratio can be checked with chart values of Ref. [12].

Hoses and tube in brake system are under pressure and their volume increases. According to empirical studies [12] there the volume changes in hoses and tubes of the brake system can be estimated as:

$$\Delta v = p_L \, L \, r^3 \left(\frac{\pi}{2} + 2\pi\left(1 - \frac{3v}{2}\right)\right)/E_t$$

where p_L is the pressure of the liquid, L is the length of the tube, r is tube radius, v is Poisson's ratio of the tube and E_t is the elastic modulus of the tube, which is usually made of steel.

We can use the following Equation to calculate the volume of liquid:

$$v_{ml} = K_H L_r \; p_L$$

in which KH = 4.39 $*10^{-6}$. The main cylinder leak-out which depends on the size of the tube and fluid pressure is calculated as:

$$\Delta v_{ml} = K_{mc} \; p_L$$

The ratios of the leakage coefficient related to various tube sizes are listed in Table 4.

Considering that the brake disc temperature must cool down to below 100°C, we can calculate the rate of heat transfer to the disc using Equation 39:

$$\dot{q} = (A_{piston} \, p_{piston} \, V)/A_{pad}$$

where V is vehicle speed, p_{piston} is piston pressure and A_{piston} is piston surface. Energy loss per disc can be calculated as:

$$Q = 1/4 \; m \; v^2 X_i$$

Finally, we can find the brake pads' surface area as:

$$A_{pad} = \int \phi r dr = \phi(r_o^2 - r_i^2)/2$$

where ϕ is the angle of the brake pads, hence we can calculate pad surface area.

The maximum permissible pressure for the brake system's hoses are defined in ISIRI 19727 standard, and shall not exceed the values listed in Table 5. Hydraulic brake hose must withstand hydrostatic pressure up to 4000 psi for two minutes without rupture. A suitable hose is able to survive cold weather as low as 4°C and also high temperatures near 1000°C for 70 hours and must be resistive to brake oil friction.

Table 4. Ratio related to coefficients of leakage

Diameter, mm	Kmc, cm^3/n/ cm^2
19.05	150
23.8	190
25.4	220
38.1	450

[Downloaded from ce.iust.ac.ir on 2026-06-14]

[DOI: 10.22068/ijae.7.4.2571]

Table 5. The maximum tolerable pressure Pt (in 1000 psi) of hydraulic brake hose

Inside diameter	Regular expansion hose	Low expansion hose	Regular expansion hose	Low expansion hose
Up to 3 mm	0.66	0.33	1.19	0.63
4 to 5 mm	0.86	0.55	1.53	1.08
Over 6 mm	1.04	0.82	1.95	1.76

Table 6. Results of braking system force and torque calculations

Description	Parameter	Value
Static front axle normal load	p_1	9210 N
Static rear axle normal load	p_2	6436 N
Dynamic front axle normal load (at z=0.4)	N_1	12565 N
Dynamic rear axle normal load (at z=0.4)	N_2	3142 N
Front/rear axles braking force ratio (at z=0.4)	$\frac{X_1}{X_2}$	$\frac{0.79}{0.21}$
Dynamic normal reaction at the road surface for DOW and GVW (at $z_{critical}$=0.6)	N_1	DOW 15647 N GVW 18541 N
Braking force ratio for DOW (at $z_{critical}$=0.6)	$\frac{X_1}{X_2}$	$\frac{0.82}{0.18}$ DOW
Braking force ratio for GVW (at $z_{critical}$=0.6)	$\frac{X_1}{X_2}$	$\frac{0.80}{0.20}$ GVW
Longitudinal load transfer for front (at $z_{critical}$=0.6)	p_f	12630 N
Longitudinal load transfer for rear (at $z_{critical}$=0.6)	p_r	3016 N
Average amount of brake's disk for front wheels	r_{r_f}	315 mm
Average amount of brake's disk for rear wheels	r_{r_R}	311 mm
Maximum torque for front wheels	τ_{w1}	778.75 Nm
Maximum torque for rear wheels	τ_{w2}	204.38 Nm
Front axle instantaneous angular velocity	ω_1	222.22
Rear axle instantaneous angular velocity	ω_2	225.08

Table 7. Results of power dissipation calculations and ventilated brake disc design

Description	Parameter	Value
Rate of energy dissipation for front axle	$\dot{Q}_1$	173053.8
Rate of energy dissipation for rear axle	$\dot{Q}_2$	46001.9
Total energy dissipation for front	Q_1	7779.2
Total energy dissipation for rear	Q_2	29264.8
Inner/outer radius ratio of brake disc	$\frac{r_o}{r_i}$	$1.4 \leq 1.5$
Effective radius of rubbing path	r_e	110 mm
Outer radius of rubbing path	r_o	130 mm
Inner radius of rubbing path	r_i	90 mm
Friction surface area of the disc	A_s	0.028 m^2
Brake factor	$BF=2\mu$	0.84
Inner and outer pad clamp forces	$p_a= N_{c1}=N_{c2}=N_c$	1962.5 N
Threshold pressure	p_t	0.08 MPa
Inner and outer pad clamp forces	p_a	14762 N
Wheel brake torque	τ_w	2558 Nm

[Downloaded from ce.iust.ac.ir on 2026-06-14]

[DOI: 10.22068/ijae.7.4.2571]

Table 8. Application of digital logic method to material selection for brake disc

Decision Numbers	1	2	3	4	5	6	7	8	9	10	Total Score	Weight Factor (α)
Compressive Strength	0	0	1	1							2	0.2
Friction coefficient	1				0	1	1				3	0.3
Wear resistance		1			1			0	1		3	0.3
Thermal capacity			0			0		1		0	1	0.1
Density				0			0		0	1	1	0.1

Table 9. Scaled values and performance index for the material properties of candidate materials

Property	1	2	3	4	5	Performance Index (γ)	Rank
Weight	0.2	0.3	0.3	0.1	0.1		
Material	Compressive Strength (MPa)	Friction coefficient	Wear rate ($10^{-6}mm^3/Nm$)	Specific heat C_p (KJ/Kg.K)	Density (ton/m^3)		
GCI	99.5	93.2	100	46.9	37.5	86.3	1
Ti-6Al-4V	82.3	77.3	95.9	59.2	61.1	80.5	3
TMC	100	70.5	28.8	52.0	57.7	60.8	5
AMC1	31.2	79.5	72.6	100	100	71.9	4
AMC2	58.5	100	81.1	93.9	96.4	85.1	2

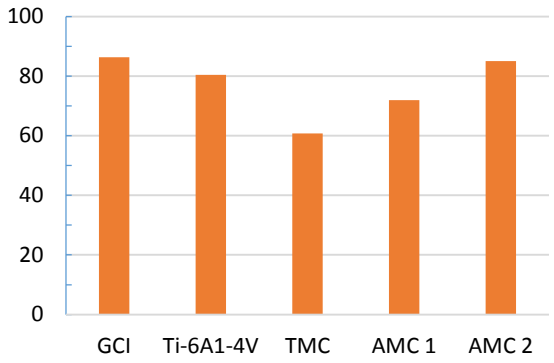

Fig9. Performance index of candidate materials for the brake disc

Table 10. Results of booster calculations and brake pedal, pad and cylinder design

Description	Parameter	Value
Brake lever ratio	R_p=(a/b)	4.3
Boost factor	B	5
Master cylinder surface area	A_{mc}	$5.64 \times 10^{-4}\ m^2$
Minimum input force (master cylinder)	P_{mc}	2000 N
Maximum input force (master cylinder)	P_{mc}	10 000 N
Master cylinder maximum pressure	P	16 MPa
Brake pad angle	ϕ	60° = π/3 rad
Brake pad surface (one pad)	A_{pad}	9 215 mm^2

[Downloaded from ce.iust.ac.ir on 2026-06-14]

[DOI: 10.22068/ijae.7.4.2571]

3. RESULTS AND DISCUSSION

Axle load calculations were performed in static conditions and dynamic braking. Then the ratio of braking forces in front and rear axles, considering the situation in which both wheels become locked at the same time was calculated and the brake force distribution ratio (X_1/X_2) was determined. Next, the brake force distribution ratio and the dynamic normal axle loads were calculated for a critical braking rate of $Z_{critical} = 0.6$, for driver-only weight (DOW) and also for gross vehicle weight (GVW).

To calculate the maximum braking torque of each wheel, rolling (or dynamic) radii of the front and rear tires were calculated and the axle braking force Ti at the tire/road interface followed by the maximum brake torque τwi is calculated. The above-calculated values are summarized in Table 6 for the braking system of the selected vehicle.

Next, the energy dissipation rate and the amount of dissipated energy per wheel on each axle is calculated. The above values are used to estimate the inner and outer radii of the brake disc and then, the inner to outer radius ratio of the disc is compared to the suggested value for good practice. Then, the dimensions of the pad and the effective radius of the disc brake are calculated, followed by the friction surface area of the disc. The friction drag force acting on the pads and the torque τw generated by a disc brake are calculated. Finally, the actuation pressure, the actuation force and axle brake torque τaxle are calculated. These values are listed in Table 7.

In the next step, digital logic method was employed, in which the comparative importance of the properties is shown in Table 8, which leads to the calculation of their respective weight factor (αi).

Then, each of the material properties of the candidate materials were scaled and the scaled values (β_i) and the weight values (α_i) were used to calculate material performance index (γ) for each candidate material, the results of which are shown in Table 9.

The performance index (γ) of the candidate materials are presented in Figure 9, which shows that gray cast iron (GCI) is the best option for application in the brake disc, followed by AMC2 (20% SiC reinforced Al-Cu alloy) and titanium alloy (Ti-6Al-4V).

Considering a minimum pedal input force of 100 N and a maximum force of 500 N, and with respect to pedal geometry, the lever ratio of the brake, the additional force exerted by the booster, the boost factor, and master cylinder surface area, input force and pressure are calculated, the values of which are summarized in Table 10.

4. CONCLUSIONS

The performance of brake system is an essential indicator of vehicle performance and directly affects other properties of the vehicle. In this paper, an introduction to brake system design for sports cars was given and the basic design and operation principles of the brake system were summarized. Basic analysis methods were explained for the calculations based on geometrical design parameters. Finally, a detailed study of a specific brake system was designed for Mercedes-AMG SLC-43, including component design parameters, operation, and braking system layout design process. A main purpose of the present work was to apply digital logic method to the material selection procedure among the candidate material proposed for brake components and to rank the materials according to performance indices. The procedure laid out in this work can be applied to the design of other vehicle systems, in future research.

[Downloaded from ce.iust.ac.ir on 2026-06-14]

[DOI: 10.22068/ijae.7.4.2571]

References

[1]. Talati F, Jalalifar S. Analysis of heat conduction in a disc brake system. Heat and mass transfer. 2009; 45(8): 1047.

[2]. Ganji HF, Ganji DD. Effects of equilibrium point displacement in limit cycle oscillation amplitude, critical frequency and prediction of critical input angular velocity in minimal brake system. AIP Advances. 2017; 7(4): 045102.

[3]. Phatak A, Kulkarni P. Drum Brake Backplate Analysis and Design Modification to Control Squeal Noise, International Journal of Engineering Development and Research. 2017; 5(3): 920-928.

[4]. Romero J, Queipo N. Reliability-based and deterministic design optimization of a FSAE brake pedal: a risk allocation analysis. Structural and Multidisciplinary Optimization. 2017; 56(3): 681-695.

[5]. Mercedes-Benz, SLC-Class Brochure, 2017.

[6]. Day A. Braking of road vehicles. Butterworth-Heinemann; New York: 2014.

[7]. Ashby MF. Materials selection in mechanical design. MRS Bull. 2005; 30(12): 995.

[8]. Shanian A, Milani AS, Carson C, Abeyaratne RC. A new application of ELECTRE III and revised Simos' procedure for group material selection under weighting uncertainty. Knowledge-Based Systems. 2008; 21(7): 709-720.

[9]. Jahazi M, Hossein-Nejad S. The development of an optimum manufacturing and material selection process for the fabrication of labyrinth seal strips. Journal of Materials Processing Technology. 2004; 152(3): 272-275.

[10]. Sapuan SM, Jacob MS, Mustapha F, Ismail N. A prototype knowledge-based system for material selection of ceramic matrix composites of automotive engine components. Materials & design. 2002; 23(8): 701-708

[11]. Zhu F, Lu G, Zou R. On the development of a knowledge-based design support system for energy absorbers. Materials & Design. 2008; 29(2): 484-91.

[12]. Maleque, M., S. Dyuti, and M. Rahman. Material selection method in design of automotive brake disc. In: World Congress on Engineering 2010, 30 June to 2 July 2010, London, United Kingdom: 1196-1201.

[Downloaded from ce.iust.ac.ir on 2026-06-14]

[DOI: 10.22068/ijae.7.4.2571]